P2mit

NASA TECHNICAL NOTE

NASA TN D-7668

AN INVESTIGATION OF THE FACSIMILE
CAMERA RESPONSE TO OBJECT MOTION

by Friedrich O. Huck, Stephen D. Wall,
and Ernest E. Burcher

Langley Research Center
Hampton, Va. 23665

NATIONAL AERONAUTICS AND SPACE ADMINISTRATION • WASHINGTON, D. C. • JULY 1974

1. Report No. NASA TN D-7668	2. Government Accession No.	3. Recipient's Catalog No.
4. Title and Subtitle AN INVESTIGATION OF THE FACSIMILE CAMERA RESPONSE TO OBJECT MOTION		5. Report Date July 1974
		6. Performing Organization Code
7. Author(s) Friedrich O. Huck, Stephen D. Wall, and Ernest E. Burcher		8. Performing Organization Report No. L-9516
9. Performing Organization Name and Address NASA Langley Research Center Hampton, Va. 23665		10. Work Unit No. 815-20-04-03
		11. Contract or Grant No.
12. Sponsoring Agency Name and Address National Aeronautics and Space Administration Washington, D.C. 20546		13. Type of Report and Period Covered Technical Note
		14. Sponsoring Agency Code

15. Supplementary Notes

16. Abstract

Motion degradation in images obtained with frame cameras (e.g., film and storage television cameras) has received considerable attention but has been of little concern for scanning cameras (e.g., conventional television cameras and optical-mechanical scanners). Some recent applications of optical-mechanical scanning techniques in facsimile cameras for planetary lander missions, however, have emphasized the spatial characterization of the scene and possible object motion in the scene.

A general analytical model of the facsimile camera response to object motion is derived as an initial step toward characterizing the resulting image degradation. This model expresses the spatial convolution of a time-varying object radiance distribution and camera point-spread function for each picture element in the image. Time variations of these two functions during each convolution account for blurring of small image detail, and variations between, as well as during, successive convolutions account for geometric image distortions. If the object moves beyond the angular extent of several picture elements while it is being imaged, then geometric distortion tends to dominate blurring as the primary cause of image degradation. The extent of distortion depends not only on object size and velocity but also on the direction of object motion, and is therefore difficult to classify in a general sense.

17. Key Words (Suggested by Author(s)) Facsimile camera Optical-mechanical scanner Motion degradation	18. Distribution Statement Unclassified – Unlimited STAR Category 14

19. Security Classif. (of this report) Unclassified	20. Security Classif. (of this page) Unclassified	21. No. of Pages 25	22. Price* $3.00

AN INVESTIGATION OF THE FACSIMILE CAMERA
RESPONSE TO OBJECT MOTION

By Friedrich O. Huck, Stephen D. Wall,
and Ernest E. Burcher
Langley Research Center

SUMMARY

Motion degradation in images obtained with frame cameras (e.g., film and storage television cameras) has received considerable attention but has been of little concern for scanning cameras (e.g., conventional television cameras and optical-mechanical scanners). Some recent applications of optical-mechanical scanning techniques in facsimile cameras for planetary lander missions, however, have emphasized the spatial characterization of the scene and possible object motion in the scene.

A general analytical model of the facsimile camera response to object motion is derived as an initial step toward characterizing the resulting image degradation. This model expresses the spatial convolution of a time-varying object radiance distribution and camera point-spread function for each picture element in the image. Time variations of these two functions during each convolution account for blurring of small image detail, and variations between, as well as during, successive convolutions account for geometric image distortions. If the object moves beyond the angular extent of several picture elements while it is being imaged, then geometric distortion tends to dominate blurring as the primary cause of image degradation. The extent of distortion depends not only on object size and velocity but also on the direction of object motion, and is therefore difficult to classify in a general sense.

INTRODUCTION

The general function of an imaging system is to translate variations in object radiance into an image or an electrical signal from which an image can be constructed. Imaging systems may accomplish this function by employing either one of two basic mechanisms. Some imaging systems, referred to as frame cameras, sense all picture elements of an object simultaneously (e.g., film and storage television cameras). Other imaging systems, referred to as scanning cameras, sense all picture elements time sequentially (e.g., conventional television cameras and optical-mechanical scanners).

A common source of image-quality degradation for all these cameras is relative motion between object and camera during image acquisition. Although motion degradation in images obtained with frame cameras has received considerable attention, primarily because of the past applications of these devices in military reconnaissance, this source of degradation has been of little concern in scanning cameras. This lack of concern in conventional television cameras can be traced to their past application to obtain motion pictures, in which the most visible effect of too rapid object motion is motion distortion in successive frames rather than image degradation in individual frames; a familiar example of motion distortion is the apparent reverse rotation of wagon wheels. The same lack of concern in optical-mechanical scanners can be traced to their past application primarily to characterize spectral or radiometric variations in scene radiance rather than spatial detail. However, recent applications of optical-mechanical scanning techniques in facsimile cameras for planetary landers emphasize the spatial characterization of the scene and possible object motion in the scene.

A general analytical model of the facsimile camera response to object motion is therefore derived in this paper as an initial step toward characterizing the resulting image degradation. To the extent that this model is independent of the specific facsimile camera scanning configuration, it is applicable also to scanning cameras in general. Several approximations to this model are introduced in order to obtain a greatly simplified expression which, in turn, is used to predict first-order image degradations caused by linear object motion. These predictions are experimentally tested with a facsimile camera.

SYMBOLS

$A(\chi,\psi)$ camera field of view, sr

$H(\chi,\psi)$ radiance distribution in image plane, W/sr

$I(\chi,\psi)$ photosensor output current, A

$I_s(\chi,\psi)$ sampled photosensor output current, A

$L(\chi,\psi)$ lens point-spread function

m azimuth step or line-scan count (fig. 3)

M number of azimuth steps or line scans per frame (fig. 3)

n	vertical sample count (fig. 3)
N	number of active samples per line scan (fig. 3)
$O(\chi,\psi)$	spatial distribution of object radiance, W/sr
$P(\chi,\psi)$	point-spread function of photosensor aperture
$R(\lambda)$	photosensor responsivity, A/W
$S(\chi,\psi)$	camera point-spread function
$t(m,n)$	time, sec (see eq. (5))
u	radial coordinate axis
u_0	radial object distance, m (fig. 4)
u_0'	initial radial object distance, m
$\dot{u}_0$	radial object velocity, m/sec
Δu	variable for defocus as a function of object distance
X	vertical sampling interval, rad
Y	azimuth sampling interval, rad
z	optical axis
δ	unit impulse function
η	line scan efficiency
λ	wavelength
$\tau(\lambda)$	transmissivity of camera optics
χ	vertical angle of lens coordinates, rad (fig. 2(b))

χ_s	vertical angle of mirror scanning coordinates, rad (fig. 2(a))
$\dot{\chi}_s$	vertical angular scanning rate, rad/sec (fig. 4)
χ_o	vertical angular object position, rad (fig. 4)
$\dot{\chi}_o$	vertical angular object velocity, rad/sec
ψ	azimuth angle of lens coordinates, rad (fig. 2(b))
ψ_s	azimuth angle of mirror scanning coordinates, rad (see fig. 2(a))
$\dot{\psi}_s$	azimuth angular stepping rate, rad/sec (fig. 4)
ψ_o	azimuth angular object position, rad (fig. 4)
$\dot{\psi}_o$	azimuth angular object velocity, rad/sec
Ψ	azimuth angular stepping interval, rad
$\Pi(\chi)$	rectangle function; 1 when $\left|\chi\right| \leq \frac{1}{2}$; 0 otherwise
$\Pi(\chi, \psi)$	two-dimensional rectangle function; 1 when $\left|\chi\right| \leq \frac{1}{2}$ and $\left|\psi\right| \leq \frac{1}{2}$; 0 otherwise $\left(\Pi(\chi, \psi) = \Pi(\chi)\Pi(\psi)\right)$
$\text{III}(\psi)$	sampling or comb function, $\displaystyle\sum_{n=-\infty}^{\infty} \delta(\psi-n)$

$$\text{III}(\chi,\psi) = \text{III}(\chi)\ \text{III}(\psi) = \sum_{n=-\infty}^{\infty}\sum_{m=-\infty}^{\infty} \delta(\chi-n, \psi-m)$$

GENERAL ANALYTICAL MODEL

An analytical model of the facsimile camera response to object motion is derived by first defining all time-dependent terms of a model which accounts for a stationary object field, and then explicitly formulating object motion.

Stationary Object Field

Imaging process.- A basic configuration of the facsimile camera is illustrated in figure 1. Radiation from the object field is reflected by the scanning mirror, captured

Azimuth rotation axis

Vertical scan mirror

Vertical scan axis

Window
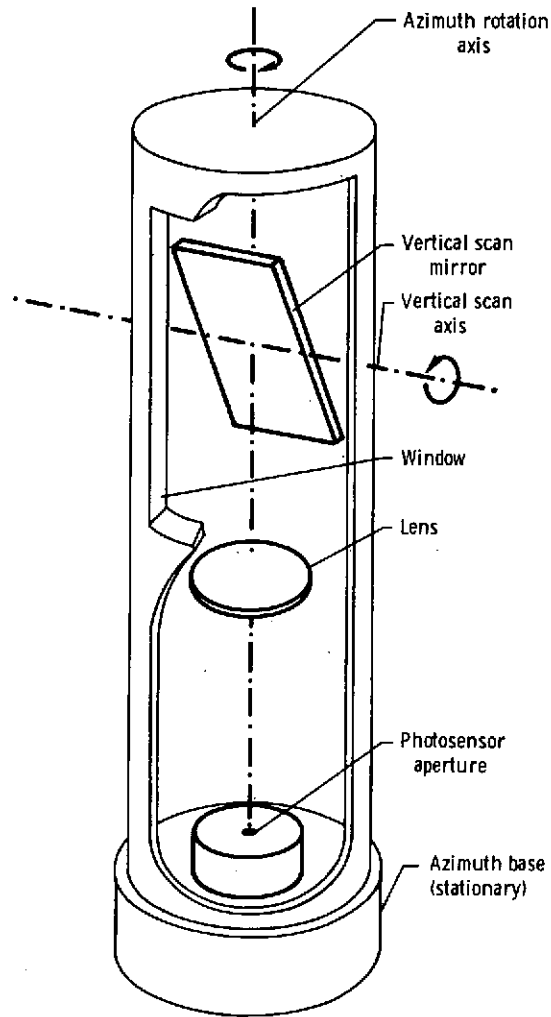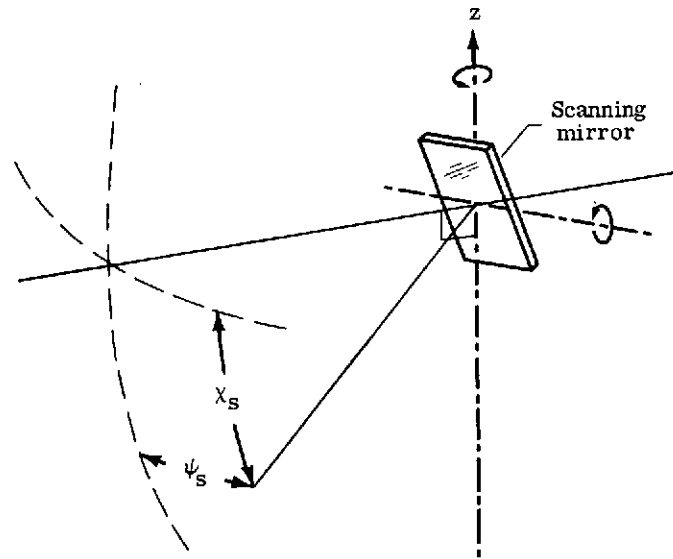
Lens

Photosensor aperture

Azimuth base (stationary)

Figure 1.- Basic facsimile camera configuration.

by the objective lens, and projected onto a plane which contains a photosensor aperture. The photosensor converts the radiation falling on the aperture into an electrical signal which is then amplified and sampled for digital transmission. As the mirror rotates, the imaged object field moves past the aperture and thus permits the aperture to scan vertical strips. The camera rotates in small steps between each vertical line scan until the entire object field of interest is scanned.

Two coordinate systems must be accounted for, as illustrated in figure 2. One coordinate system with an origin at the center of the mirror (fig. 2(a)) accounts for the

(a) Scanning geometry.
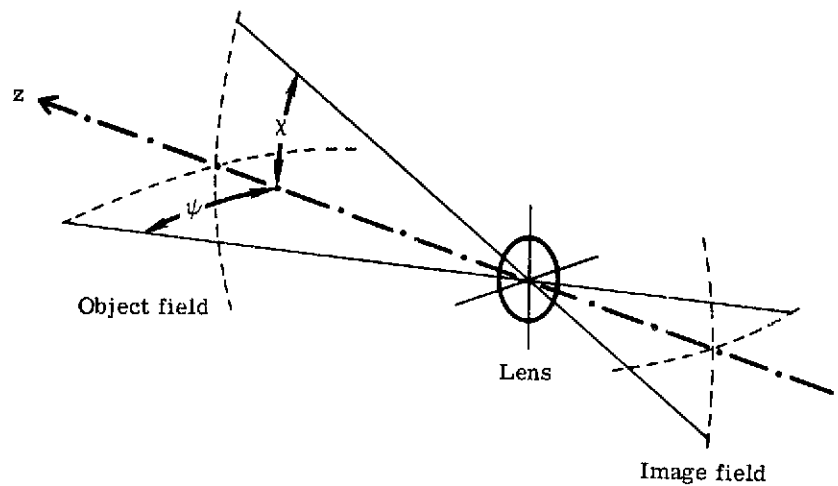
(b) Image-forming geometry.

Figure 2.- Camera coordinate system.

camera scanning geometry, and the other coordinate system with an origin at the center of the lens (fig. 2(b)) accounts for the imaging geometry. The vertical angle through which the mirror has scanned the object field is labeled χ_s, and the azimuth angle through which the camera has rotated is labeled ψ_s. The vertical angle χ_s is measured from a plane normal to the axis of azimuth rotation (i.e., from the horizon), and the

azimuth angle ψ_s is measured in this plane from an arbitrary reference angle. The axis of azimuth rotation is also the optical axis of the objective lens and is labeled z in figure 2. The location of an object point (with the mirror optically unfolded) and the corresponding image point is measured as an angle from this common axis at the center of the objective lens. One angle, measured along the direction in which the imaged object field is moved by the scanning mirror, is labeled χ, and the other angle, measured normal to this direction, is labeled ψ. It should perhaps be emphasized for clarity that the angles χ_s (fig. 2(a)) and χ (fig. 2(b)) occur in the same plane, but that the angles ψ_s (fig. 2(a)) and ψ (fig. 2(b)) occur in planes which are normal to each other.

The photosensor aperture is always located at or near the optical axis, so that only small (χ, ψ) angles are of interest; thus, $(\tan \chi, \tan \psi) \approx (\chi, \psi)$. It is assumed that the lens-to-mirror distance is very small compared with the mirror-to-object distance; thus, the angles χ_s and χ are interchangeable, and the angles ψ_s and ψ are related by $\psi = \psi_s \cos \chi_s$.

The transfer of the spatial radiance distribution of an object $O(\chi, \psi; \lambda)$, which is captured by the objective lens, to an image in the photosensor aperture plane may be expressed by the convolution (ref. 1)

$$H(\chi, \psi; \lambda, \Delta u) = \iint_A O(\chi - \chi', \psi - \psi'; \lambda) \, L(\chi', \psi'; \Delta u) d\chi' \, d\psi' \tag{1}$$

where $L(\chi, \psi)$ is the lens point-spread function and $A \equiv A(\chi, \psi)$, the camera field of view. The variable Δu accounts for possible defocus blur (ref. 2), which is dependent on the actual object distance from the camera relative to the object distance which is in focus.

The effect of the scanning mirror is to shift the imaged object field over the photosensor aperture plane, and the effect of the camera rotation between line scan is to advance the image in integral steps normal to the shifting direction. The process by which the photosensor converts this radiant power into an electrical signal may be formulated as

$$I(\chi, \psi; \Delta u) = \int_0^\infty \iint_A \tau(\lambda) \, R(\lambda) \, H(\chi - \chi', \psi - \psi'; \lambda, \Delta u) \, P(\chi', \psi') d\chi' \, d\psi' \, d\lambda \, \frac{1}{Y} \, \mathrm{III}\left(\frac{\psi}{Y}\right) \tag{2}$$

where $\tau(\lambda)$ is the transmissivity of the optical path in the camera; $R(\lambda)$, the responsivity of the photosensor; and $P(\chi, \psi)$, the point-spread function of the photosensor aperture. The symbol $\mathrm{III}\left(\frac{\psi}{Y}\right)$ is the sampling (ref. 3) or comb (ref. 4) function; this function is essentially an infinite sum of delta functions whose spacings in this case are related to the azimuth angular stepping interval Ψ by $Y = \Psi \cos \chi_s$.

The electrical signal generated along the vertical line-scan direction is generally sampled for digital transmission. The effective vertical angular sampling interval is expressed here by X. The possible effect of electronic transfer characteristics on the video signal, other than sampling, is neglected. The imaging process of the facsimile camera may then be written as

$$I_s(\chi,\psi;\Delta u) = \int_0^\infty \iiiint_A \tau(\lambda)\,R(\lambda)\,O(\chi-\chi',\psi-\psi';\lambda)\,L(\chi'-\chi'',\psi'-\psi'';\Delta u)\,P(\chi'',\psi'')d\chi''\,d\psi''\,d\chi'\,d\psi'\,d\lambda\,\frac{1}{XY}\,\text{III}\!\left(\frac{\chi}{X},\frac{\psi}{Y}\right) \qquad (3)$$

Only the spatial characteristics of the imaging process are of interest to this analysis, so that the spectral radiance transfer characteristics can be neglected and equation (3) can be reduced to

$$I_s(\chi,\psi;\Delta u) = \iint_A O(\chi-\chi',\psi-\psi')\,S(\chi',\psi';\Delta u)d\chi'\,d\psi'\,\frac{1}{XY}\,\text{III}\!\left(\frac{\chi}{X},\frac{\psi}{Y}\right) \qquad (4)$$

where $S(\chi,\psi;\Delta u)$ is the camera point-spread function

$$S(\chi,\psi;\Delta u) = \iint_A L(\chi-\chi',\psi-\psi';\Delta u)\,P(\chi',\psi')d\chi'\,d\psi'$$

The foregoing formulation of the imaging process for facsimile cameras is identical with those for frame cameras except for the sampling function. This equation may be evaluated by first convolving the object radiance distribution with the camera point-spread function over the entire camera field of view and then sampling the resulting distribution at intervals determined by the sampling function. The sampling function does not alter the information content of the signal if the sampling intervals are sufficiently small compared with the smallest object detail passed by the camera point-spread function. Nor does the sampling function distort the location of any picture elements (pixels). Consequently, if the signal is properly reconstructed on a storage medium, such as film, without introducing any degradation, then the resultant image would not differ measurably from an image obtained with a framing camera which has the same point-spread function.

Time dependence.- The imaging process just formulated is implicitly a function of time for scanning cameras; that is, $\chi = \chi(t)$ and $\psi = \psi(t)$. As long as the object is stationary, this time dependence translates into a time dependence of the electrical signal $I_s(\chi,\psi)$ which is removed again when this signal is recorded as an image. However, as soon as the object moves, this time dependence becomes important.

Several assumptions and definitions are made in order to formulate the time dependence of the scanning mechanism of the facsimile camera:

(1) A complete mirror line scan consists of an active and inactive period. During the active period, the mirror scans the object field of interest at a constant rate $\dot{\chi}_s$. During the inactive period, the mirror returns to the initial active scan position. The ratio of the active scan period to the complete scan period is defined as scanning efficiency η.

(2) The camera rotates one step in azimuth during each inactive mirror scan period at an average rate $\dot{\psi}_s$.

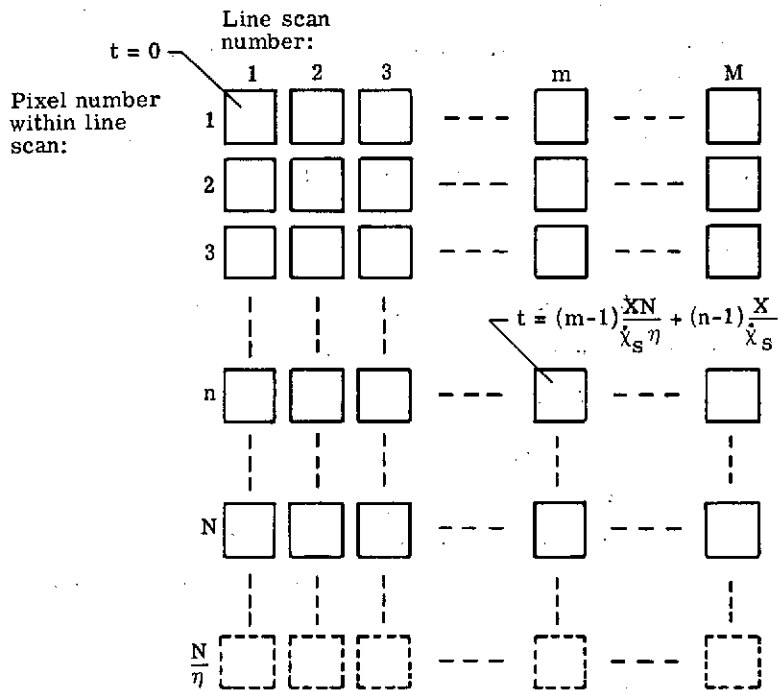(3) A complete image contains M scan lines and N pixels per line, as illustrated in figure 3.

Figure 3.- Illustration of image containing M scan lines and N pixels per line.

Consequently, the time to complete a mirror line scan is $\dfrac{\Psi}{\dot{\psi}_s} = \dfrac{XN}{\dot{\chi}_s \eta}$; the active part of this scan, $\dfrac{X}{\dot{\chi}_s}N$; and the inactive part, $\dfrac{XN}{\dot{\chi}_s \eta}(1 - \eta)$. It can be seen from figure 3 that the time required to reach the nth pixel in the mth line is

$$t \equiv t(m,n) = \frac{X}{\dot{\chi}_s}\left[\frac{N}{\eta}(m - 1) + (n - 1)\right] \tag{5}$$

With these assumptions and definitions, equation (4) may be rewritten explicitly as a function of time as

$$I_S\left[M,N;\chi(t),\psi(t);\Delta u\right] = \int_0^{YM}\int_0^{XN} O\left[\chi(t)-\chi',\psi(t)-\psi'\right] S(\chi',\psi';\Delta u)d\chi'\,d\psi' \sum_{m=1}^{M}\sum_{n=1}^{N/\eta} \delta\left[\chi(t)-Xn,\psi(t)-Ym\right] \quad (6)$$

where $\chi(t) = \dot{\chi}_s t$ and $\psi(t) = \dot{\psi}_s t \cos\dot{\chi}_s t$, and the camera field of view (for a single frame) $A \equiv A(\chi,\psi)$ is replaced by $(XN)(YM)$. This expression, unlike that of equation (4), cannot generally be evaluated by first convolving the object radiance distribution $O(\chi,\psi)$ with the camera point-spread function $S(\chi,\psi)$ and then sampling the resulting distribution. Instead, this expression must generally be evaluated by convolving $O(\chi,\psi)$ with $S(\chi,\psi)$ at each instant of time $t \equiv t(m,n)$ (i.e., for each pixel) for a total of MN convolutions. The summation is intended to account for the proper time sequence of the spatial location of the pixel brightness level obtained from each one of the convolutions. However, if neither $O(\chi,\psi)$ nor $S(\chi,\psi)$ varies with time, then all MN convolutions are identical and equation (6) reduces to equation (4).

Object Motion

In order to formulate the effect of object motion, it is assumed that only one object is present. This simplification avoids such problems as discrimination between moving object and stationary scene and obscuration of one object by another.

The components of object position are expressed in the mirror scanning coordinate system illustrated in figure 4. The three components become the angular position $\chi_0(t)$ along the vertical line scan direction, the angular position $\psi_0(t)$ along the azimuth direction, and the distance $u_0(t)$ radially outward from the camera. Object motion can then be included in equation (6) as follows:

$$I_S\left[M,N;\bar{\chi}(t),\bar{\psi}(t),\bar{u}(t);\Delta u(t)\right] = \int_0^{YM}\int_0^{XN} O\left[\frac{\bar{\chi}(t)-\chi'}{\bar{u}(t)},\frac{\bar{\psi}(t)-\psi'}{\bar{u}(t)}\right] S\left[\chi',\psi';\Delta u(t)\right] d\chi'\,d\psi' \sum_{m=1}^{M}\sum_{n=1}^{M/\eta} \delta\left[\chi(t)-Xn,\psi(t)-Ym\right] \quad (7)$$

where

$$\bar{\chi}(t) = \dot{\chi}_s t - \chi_0(t)$$

$$\bar{\psi}(t) = \left[\dot{\psi}_s t - \psi_0(t)\right]\cos\dot{\chi}_s t$$

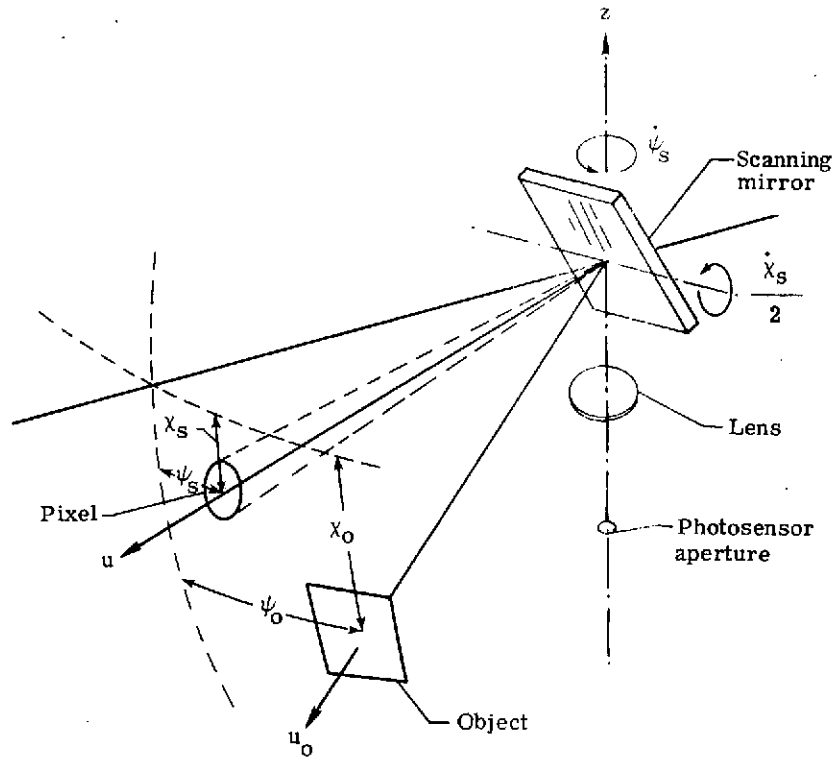$$\bar{u}(t) = 1 - \frac{u_0(t)}{u_0'}$$

10

Figure 4.- Facsimile camera scanning geometry and object motion.

The time dependence of the angular object position $\chi_0(t)$ and $\psi_0(t)$ accounts for the fact that the camera point-spread function slides past the moving object either faster or slower than past a stationary object, depending on the direction and rate of the object motion with respect to the scanning motion.

The time dependence of the object distance $u_0(t)$ accounts for the fact that the apparent angular extent of the object increases or decreases in size compared with the camera point-spread function, depending on the direction of the radial object motion. Furthermore, the time dependence of defocus blur $\Delta u(t)$ causes the shape of the camera point-spread function to change with time. The parameter u_0' is the distance between object and camera when the first pixel is sensed, that is, when $m = 1$, $n = 1$, and $t = 0$; $u_0(t) = 0$ when $t = 0$.

As has been noted before, this formulation requires the convolution of the object radiance distribution with the camera point-spread function at each instant of time $t = t(m,n)$, or, in other words, for each pixel in the image. It may also be noted that both these functions may change during and between each one of the convolutions.

The time dependence during convolution may be recognized to occur also in frame cameras, except that it occurs there for all pixels simultaneously. Consequently, each individual convolution can be evaluated by means of techniques developed for frame

11

cameras. (See, e.g., ref. 5.) Furthermore, the effect on the image can be expected to appear as blurring of small detail.

The time dependence of these two functions between convolutions does not exist in frame cameras. This time dependence between, as well as during, successive convolutions may be recognized as a cause of primarily geometric distortion. If the object position changes over several pixels or more, then geometric distortion may be expected to dominate blurring of small detail as the primary effect of image degradation. Furthermore, if the object position changes beyond the field of view of the camera (for a single image frame), then the assumption can often be made that object motion is negligible during the acquisition period of a single pixel; otherwise, only a very few pixels of the object would be sensed before the object disappeared from the field of view, and then the potential for even the most rudimentary reconstruction of the object shape would generally be lost. (Incidentally, whenever this assumption can be made for frame cameras, then image degradation will also be negligible since all pixels are sensed simultaneously.)

SIMPLIFIED ANALYTICAL MODEL

The general analytical model of the facsimile camera response to object motion, as formulated by equation (7), is difficult to evaluate. Several simplifying assumptions are therefore introduced in order to reduce this model to several simpler ones which can be used more conveniently to characterize first-order effects of motion degradation:

(1) The camera field of view is small and centered around the plane normal to the axis of azimuth rotation (the horizon); that is, $\cos \chi_s \approx 1$, and the two angles ψ_s and ψ are interchangeable.

(2) The azimuth sampling interval is equal to the vertical sampling interval; that is, $Y = X$.

(3) The camera point-spread function $S(\chi, \psi)$ is approximated by the rectangle function $\Pi\left(\frac{\chi}{X}, \frac{\psi}{X}\right)$. This function defines a square instantaneous field of view of angular extent X, and ignores lens degradation and defocus blur. However, degradation due to defocus blur is small as long as the object remains within the depth of field of the camera (ref. 2).

(4) The object moves at a constant velocity; that is,

$$\chi_0(t) = \dot{\chi}_0 t \qquad \psi_0(t) = \dot{\psi}_0 t \qquad u_0(t) = \dot{u}_0 t$$

Substituting these assumptions into equation (7) yields

12

$$I_s(M,N;\dot{\chi},\dot{\psi},\dot{u}) = \int_0^{YM} \int_0^{XN} O\left[\frac{\overline{\chi}(t)-\chi'}{\overline{u}(t)}, \frac{\overline{\psi}(t)-\psi'}{\overline{u}(t)}\right] \Pi\left(\frac{\chi'}{X}, \frac{\psi'}{X}\right) d\chi' \, d\psi' \sum_{m=1}^{M} \sum_{n=1}^{N/\eta} \delta\left[\chi(t)-Xn, \psi(t)-Xm\right] \tag{8a}$$

where

$$\overline{\chi}(t) = \left(\dot{\chi}_s - \dot{\chi}_0\right) t$$

$$\overline{\psi}(t) = \left(\dot{\psi}_s - \dot{\psi}_0\right) t = \left(\frac{\eta}{N} \dot{\chi}_s - \dot{\psi}_0\right) t$$

$$\overline{u}(t) = 1 - \frac{\dot{u}_0}{u_0'} t$$

The spatial convolutions of equation (7) are now reduced to integrations of the object radiance distribution over a pixel, the size of which is determined by the product of camera instantaneous field of view and object distance from the camera at the time of integration. As before, the summation is intended to account for the proper time sequence of the spatial location of each pixel. This function of the summation may be emphasized by substituting equation (5) for the variable t:

$$I_s(M,N;\dot{\chi},\dot{\psi},\dot{u}) = \int_0^{YM} \int_0^{XN} O\left[\frac{\overline{\chi}(m,n)-\chi'}{\overline{u}(m,n)}, \frac{\overline{\psi}(m,n)-\psi'}{\overline{u}(m,n)}\right] \Pi\left(\frac{\chi'}{X}, \frac{\psi'}{X}\right) d\chi' \, d\psi' \sum_{m=1}^{M} \sum_{n=1}^{N/\eta} \delta\left[\chi(m,n)-Xn, \psi(m,n)-Xm\right] \tag{8b}$$

where

$$\overline{\chi}(m,n) = \left(1 - \frac{\dot{\chi}_0}{\dot{\chi}_s}\right) X\left[\frac{N}{\eta}(m-1) + (n-1)\right]$$

$$\overline{\psi}(m,n) = \left(\frac{\eta}{N} - \frac{\dot{\chi}_0}{\dot{\chi}_s}\right) X\left[\frac{N}{\eta}(m-1) + (n-1)\right]$$

$$\overline{u}(m,n) = 1 - \frac{\dot{u}_0}{\dot{\chi}_s u_0'} X\left[\frac{N}{\eta}(m-1) + (n-1)\right]$$

It is apparent from this simplified model that the primary effect of motion degradation in scanning cameras is geometric distortion rather than contrast reduction of fine detail as in frame cameras. This basic difference has the unfortunate consequence that existing analytical tools for evaluating motion-degraded images and computer software techniques for removing some of this degradation, which have been developed for frame cameras, are not generally applicable to scanning cameras.

ANALYTICAL AND EXPERIMENTAL RESULTS

As has been revealed by the foregoing analyses, the general model of the facsimile camera response to object motion is a very complicated function which can be simplified significantly by assuming linear object motion and approximate camera response characteristics. A computer program based on the simplified analytical model is used to simulate motion-degraded images, and these images in turn are compared with actual facsimile camera images. The computer program is described in appendix A, and the experimental facility in appendix B.

The object consists of the four letters H, O, U, and T, as illustrated in figure 5. At the initial distance u_o, each letter is 12 pixels long and 7 pixels wide, and the spacing between letters is 3 pixels. The computer prints each pixel as the character 8. Two differences between computer printout and facsimile camera images should be noted: One, the aspect ratio of the computer-simulated letters is distorted by a factor of 1.6
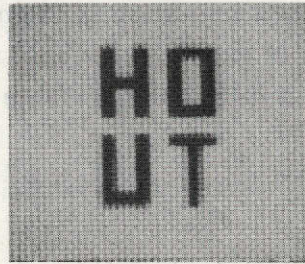
Computer printout   Facsimile camera

Figure 5.- Undegraded image.

because the spacing between characters along the computer printing line (which corresponds to the camera vertical line scan) is narrower than the spacing between lines (which corresponds to the camera azimuth steps). And two, the details of the letters in the actual image vary slightly in width and contrast because the facsimile camera inadvertently scans and samples the object in such a way that object and background are integrated within various pixels in slightly different proportions. (This occurrence is, incidentally, a result of insufficient sampling.)
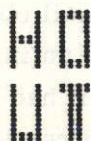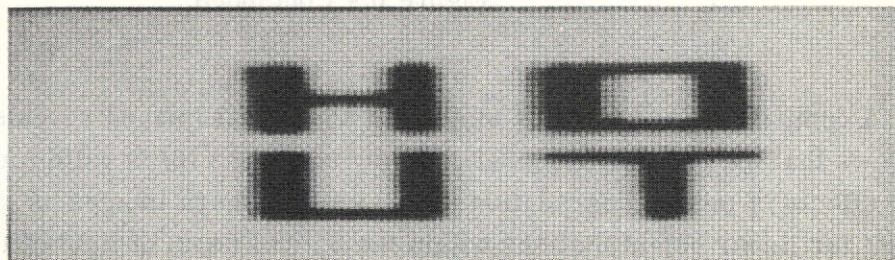
Image degradations caused by object motion, both as simulated by the computer program and as obtained with the facsimile camera, are illustrated in figure 6. Figure 6(a) presents image degradations for a vertical object velocity component opposing the line scan direction $-\dot{\chi}_o/\dot{\psi}_s$. (Vertical velocity components along the line scan direction $\dot{\chi}_o/\dot{\psi}_s$ result in similar distortions.) Figure 6(b) presents image degradations for

(a) Vertical object motion, $\dfrac{\dot{\chi}_o}{\dot{\psi}_s} = -2$.


$\dfrac{\dot{\psi}_o}{\dot{\psi}_s} = 0.8$

$\dfrac{\dot{\psi}_o}{\dot{\psi}_s} = -0.8$

(b) Azimuth object motion.

Figure 6.- Motion-degraded images.

azimuth object velocity components, both along the camera stepping direction $\dot{\psi}_o/\dot{\psi}_s$ and opposite to this direction, $-\dot{\psi}_o/\dot{\psi}_s$. And figure 6(c) presents image degradations for radial object velocity components directed toward the camera $-\dot{u}_o/u'_o\dot{\psi}_s$. (Radial object velocity components directed away from the camera $\dot{u}_o/u'_o\dot{\psi}_s$ result in similar degradations if the initial distance u'_o and the final distance are reversed.)
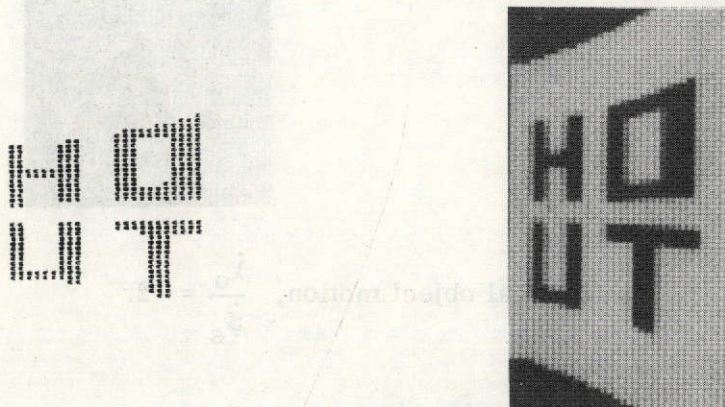
(c) Radial object motion, $\dfrac{\dot{u}_o}{u_o\dot{\psi}_s} = -6.$

Figure 6.- Concluded.

A comparison of computer simulated and actual images reveals close agreement. It follows that the simplified model given by equations (8) is valid for predicting first-order effects of motion degradation in facsimile camera images as geometric distortions, at least for linear object motions within the optical depth of field of the camera. It is difficult, however, to classify the extent of even this limited class of distortions in a general sense, as for example, by recognition limits as a function of object size and velocity. This difficulty exists because the extent of geometric distortion depends not only on object size and velocity compared with camera angular resolution and scanning rate but also on the direction of object motion. For example, a small object moving with a certain velocity in the direction of azimuth rotation may result in an image wherein this object, although distorted, may be easier to recognize than if it had been stationary, while the same object moving at the same velocity in the opposite direction may result in an image wherein the object is no longer recognizable.

CONCLUDING REMARKS

A general analytical model was derived for the facsimile camera response to object motion. This model expresses essentially the spatial convolution of a time-varying object radiance distribution and camera point-spread function for each picture element (pixel) in the image. The response of the facsimile camera and other scanning cameras which sense pixels in time sequence is therefore fundamentally different from that of frame cameras which sense all pixels simultaneously.

In order to characterize approximately the dominant response characteristics of the facsimile camera to object motion, the general analytical model was greatly simplified, primarily by assuming an approximate camera response and linear object motion. A comparison of motion-degraded images simulated by computer software and obtained with a facsimile camera revealed close agreement and led to the following conclusions:

1. First-order effects of object-motion degradation in facsimile camera images appear primarily as geometric distortions. Blurring of detail, which exists in frame cameras, is generally also present but less significant. As a consequence, existing analytical tools for evaluating motion-degraded images and computer software techniques for removing some of this degradation, which have been developed for frame cameras, are not generally applicable to scanning cameras.

2. A very simplified analytical model instead of the general model should often suffice to characterize geometric distortions in facsimile camera images.

3. It is difficult to classify the extent of geometric image distortion in a general sense as, for example, by recognition limits as a function of object size and velocity, because the extent of geometric distortion depends not only on these factors but also on the direction of object motion.

Langley Research Center
National Aeronautics and Space Administration,
Hampton, Va., May 3, 1974.

APPENDIX A

COMPUTER PROGRAM

The computer program used to predict geometric distortions in facsimile camera images as a function of object motion is based on a further approximation of the simplified model given by equation (8b).

The facsimile camera used to obtain experimental results (see appendix B for details) employs a continuously rotating scanning mirror, and thus has a very low scanning efficiency (about 10 percent). In other words, the period during which the mirror actively scans the scene is very short compared with the time required to complete a vertical scan line, or advance one pixel in azimuth. It is consequently assumed that the magnitude of object traversal during the active line-scan period is negligible. This assumption leads to a further simplification of equation (8b). The time $t(m,n)$, as given by equation (5), to reach the nth pixel in the mth line may now be replaced by the time $t(m) = \dfrac{XN}{\dot{\chi}_s \eta}(m - 1)$ required to reach the mth line.

Furthermore, it is assumed that the object radiance distribution $O(\chi, \psi)$ has a uniform radiance level (unity) and the background, another level (zero). Hence, when the instantaneous field of view of the camera scans the object, the resulting image level will be unity; when it scans the background, the image level will be zero. A range of intermediate image levels could, of course, still be generated when the instantaneous field of view samples part of the object and part of the background. This effect is eliminated by defining a threshold for the image irradiance so that

$$I\left[\bar{\chi}(m)-\chi, \ \bar{\psi}(m)-\psi; \ \bar{u}(m)\right] = 1$$

when

$$\int_0^{YM} \int_0^{XN} O\left[\frac{\bar{\chi}(m)-\chi'}{\bar{u}(m)}, \frac{\bar{\psi}(m)-\psi'}{\bar{u}(m)}\right] \Pi\left(\frac{\chi'}{X},\frac{\psi'}{X}\right) d\chi' \, d\psi' \geq \frac{1}{2}$$

and

$$I\left[\bar{\chi}(m)-\chi, \ \bar{\psi}(m)-\psi; \ \bar{u}(m)\right] = 0$$

otherwise. Or in words, the image brightness is equal to unity when part of the object fills half or more of the camera instantaneous field of view, and is equal to zero otherwise. The above integration does not, therefore, actually have to be carried out to determine image brightness levels. Equation (8b) becomes then

18

$$I_s\left(M,N;\dot{\chi}_o,\dot{\psi}_o,\dot{u}_o\right) = I\left[\bar{\chi}(m)-\chi,\ \ \overline{\psi}(m)-\psi;\ \ \bar{u}(m)\right] \sum_{m=1}^{M} \sum_{n=1}^{N/\eta} \delta\left[\chi(m,n)-Xn,\ \psi(m,n)-Xm\right]$$

where

$$\bar{\chi}(m) = \left(\frac{N}{\eta} - \frac{\dot{\chi}_o}{\dot{\psi}_s}\right) X(m-1)$$

$$\overline{\psi}(m) = \left(1 - \frac{\dot{\psi}_o}{\dot{\psi}_s}\right) X(m-1)$$

$$\bar{u}(m) = 1 - \frac{\dot{u}_o}{u'_o \dot{\psi}_o} X(m-1)$$

The computer output printer may be regarded as an image reproducer. The distance between pixels X becomes the spacing between computer printout characters. The counts n = 1 and m = 1 move the printer to the character location of the first printout line. Then each count n advances the printer along the line to the next character position. When the count n has reached the value N/η, the count m is advanced by one integer and the printer is advanced to the next line. The next count n positions the printer to the first character location in the new line. This process is repeated until the Mth line has been completed. A character is printed whenever I[ ] is unity; otherwise, no character is printed.

The term I[ ] depicts all the required computations. In essence, these computations consist of two operations. One operation shifts the object O[ ] for each count m by a distance which is determined by $\bar{\chi}(m)$ and $\overline{\psi}(m)$. The second operation enlarges or reduces the instantaneous field of view $\Pi(\ )$ by an amount which is determined by $\bar{u}(m)$. Or conversely with the same result, the second operation reduces or enlarges the object O[ ] by the same amount. If, at the instance of sampling, $\Pi(\ )$ is covered by one-fourth or more of the object area, then I[ ] = 1; otherwise, I( ) = 0.

APPENDIX B

EXPERIMENTAL FACILITY

The facility used to obtain object-motion-degraded images consists essentially of a motion simulator, facsimile camera, and image reproducer. The motion simulator and facsimile camera are shown in figure B1, and pertinent characteristics are described in this appendix. Characteristics of the image reproducer, which records the facsimile camera data on film, are not important to this investigation.

Motion Simulator

The motion simulator moves a light box with three degrees of freedom at a continuously variable rate up to 1 cm/sec. The maximum extent of travel in the forward-backward direction (which corresponds to the camera-centered radial u-coordinate axis) is 2.75 m; in the left-right direction (which corresponds to the camera-centered azimuth ψ-coordinate axis), 1.5 m; and in the up-down direction (which corresponds to the vertical χ-coordinate axis), 1.23 m.

Each of the four letters H, O, U, and T, which constitute the object, are 7.5 cm long and 4.5 cm wide; the spacing between letters is 2.0 cm.

Facsimile Camera

Camera characteristics of interest to this investigation are instantaneous field of view, depth of field, and mirror scanning rate and efficiency. These parameters are adjustable in the laboratory facsimile camera, and are given here only as used during the experiment. Pertinent characteristics of the laboratory facsimile camera are as follows:

Instantaneous field of view, deg 0.132

Diameter of objective lens, cm 1.0

Focal length of objective lens, cm 5.5

In-focus object distance, cm 180

Number of pixels per line 512

Azimuth stepping rates, $\dot{\psi}_s$:

    Rapid, deg/sec 0.04

    Slow, deg/sec 0.0145

Scanning efficiency 0.1

At the initial distance of the object from the camera u_o = 2.75 m, the object letters are about 12 pixels long and 7 pixels wide, and the spacing between letters is about 3 pixels. The depth of field (see ref. 2) ranges from 1.2 m to 3.0 m and encompasses the range of radial motion used during the experiments.
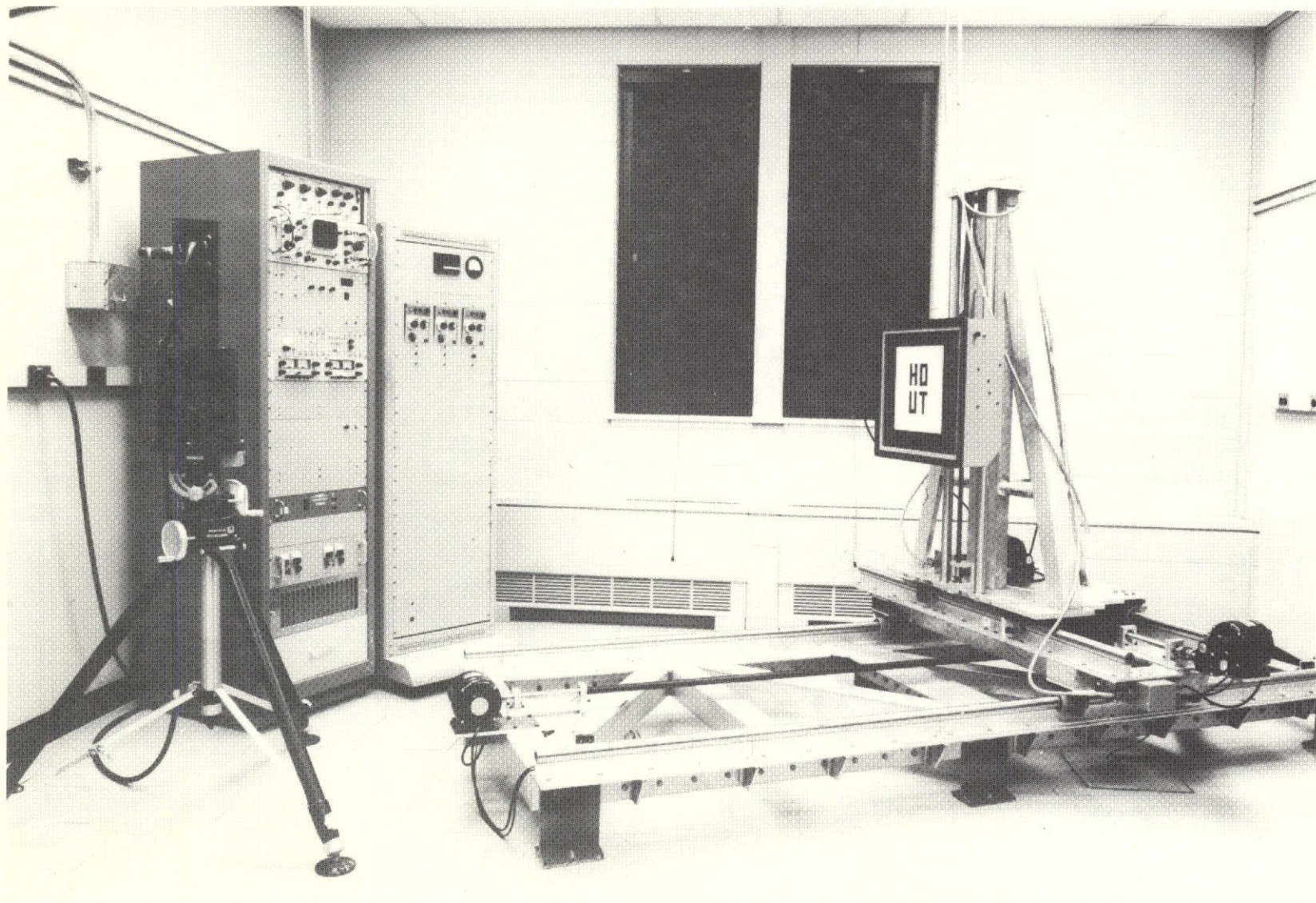
L-73-8521

Figure B1.- Experimental facility.

REFERENCES

1. Fellgett, P. B.; and Linfoot, E. H.: On the Assessment of Optical Images. Phil. Trans. Roy. Soc. London, ser. A, vol. 247, no. 931, Feb. 17, 1955, pp. 369-407.

2. Huck, Friedrich O.; and Lambiotte, Jules J., Jr.: A Performance Analysis of the Optical-Mechanical Scanner as an Imaging System for Planetary Landers. NASA TN D-5552, 1969.

3. Bracewell, Ron: The Fourier Transform and Its Applications. McGraw-Hill Book Co., c.1965.

4. Goodman, Joseph W.: Introduction to Fourier Optics. McGraw-Hill Book Co., Inc., c.1968.

5. Scott, Roderic M.: Contrast Rendition as a Design Tool. Phot. Sci. Eng., vol. 3, no. 5, Sept.-Oct. 1959, pp. 201-209.